Finite Element Evaluation of the Strength of Silicide-Based Thermoelectric Modules

A. Miozzo*[1], S. Boldrini[1], A. Ferrario[1] and M. Fabrizio[1]
[1]Institute of Condensed Matter Chemistry and Technologies for Energy – National Research Council of Italy
*Corresponding author: Corso Stati Uniti 4, 35127 Padova, Italy, alvise.miozzo@ieni.cnr.it

Abstract: Thermoelectric generation modules (TEM) are used to produce electric power from a heat flux across a temperature gradient. Silicide-based thermoelectric modules operate in mid-high temperature range. In the operating conditions, thermal stresses in materials with different coefficient of thermal expansion (thermoelectric legs, connectors, ceramic substrates) may reduce the mechanical strength of the modules. This work presents a finite element evaluation of the strength of a 16 elements silicide-based thermoelectric operating with 300 °C temperature difference. The results of the simulation have been compared with those obtained testing a module prototype.

Keywords: Thermoelectric materials, thermal stress, failure criteria

1. Introduction

Thermoelectric effects are governed by coupled nonlinear partial differential equations [1, 2, 5]. In previous works, multiphysics simulation of thermoelectric effects with COMSOL® has been performed for bismuth-telluride legs and thermocouples [1] and to evaluate output power and efficiency of mid-high silicide-based thermoelectric generators [2]. In this work, a case study of finite element evaluation of mechanical strength of a mid-high temperature operating silicide-based thermoelectric module (TEM) is presented.

Production of electrical power from heat flux across a temperature gradient is one of the applications of thermoelectric materials. In a module (TEM) for power generation, thermoelectric couples of *n*-type and *p*-type semiconductors are electrically connected in series and thermally in parallel. Maximum efficiency of a thermoelectric generator, given by

$$\eta_t = P_{max}/Q_h \qquad (1)$$

where P_{max}[W] is maximum generated electrical power and Q_h[W] is the heat flux on the hot side, generally varies between 5 – 10% for the current state-of-the-art thermoelectric materials. Considering the mean values of the thermoelectric properties for the *n*, *p*-type legs in the operating temperature range, the heat flux on the hot side can be written as follows [3]:

$$Q_h = n\left(K\Delta T + \alpha T_h I - \frac{1}{2}I^2R\right) \qquad (2)$$

being *n* the number of thermocouples. Thus, Q_h is defined as the sum of three contributions. The first one, where $K=(k_nA_n/h_n)+(k_pA_p/h_p)$ (being $k_{n,p}$ the thermal conductivity values [$Wm^{-1}K^{-1}$] and $A_{n,p}$ the cross sections [m^2] of the $h_{n,p}$ high n,p-type legs), corresponds to heat conduction with ΔT temperature gradient [K]. The second term is the thermoelectric contribution (Peltier effect), being $\alpha = |\alpha_n| + |\alpha_p|$ the Seebeck coefficient of the thermoelectric elements [V/K] and I the total current [A]. The third term is Joule heat contribution, where $R=(\rho_nh_n/A_n)+(\rho_ph_p/A_p)$ is the internal electrical resistance [Ω] (being $\rho_{n,p}$ the electrical resistivity values [Ωm]).

In this work, a 16 legs silicide-based thermoelectric module has been considered (Fig.1).

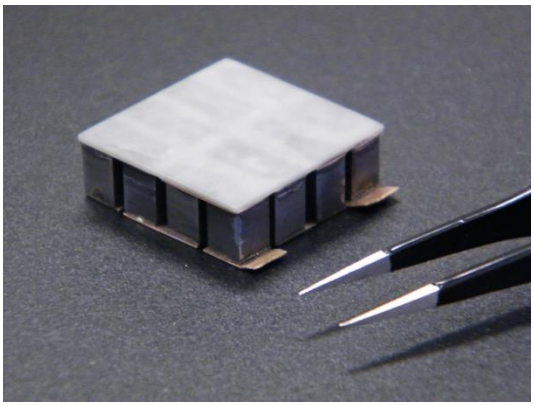

Figure 1. Prototype of the silicide-based thermoelectric module considered for the simulation.

Silicide-based thermoelectric modules provide a promising solution for thermoelectric power generation at mid-high temperatures

because of abundance, low density and low toxicity of raw constituents. In particular, modules with Sb-doped Mg_2Si *n*-type legs and Higher Manganese Silicide (HMS) *p*-type legs may operate with temperature gradients up to 500°C.

Considering a 16 legs module operating in the 50 °C – 350 °C temperature range, the mean values of the thermoelectric properties can be taken as follows [4]:

	Sb-doped Mg_2Si (*n*-type)	HMS (*p*-type)
k [$Wm^{-1}K^{-1}$]	4.74	2.39
α [μV/K]	-113	162
ρ [Ωm]	$5.7x10^{-6}$	$2.02x10^{-5}$

Table 1. Mean values of thermoelectric properties of n,p-type legs in 50°C – 350°C temperature range [4]

With these mean values and 5 x 5 x 7 mm^3 thermoelectric legs, from eq. (2) heat flux on the hot side across 300 K temperature gradient is evaluated as Q_h=68 W, of which 90% is given by the conduction term. Thus, for the sake of simplicity Peltier and Joule contributions were not considered in the simulation, that is the module was evaluated in open-circuit conditions.

Coupling materials with different thermal expansion coefficient may cause at mid-high temperature high stresses potentially undermining the mechanical strength of the modules. In particular, the material of the substrate on the hot side (Fig. 1) has to be properly chosen to limit thermal stresses.

In Table 2, the considered thermal expansion coefficient (CTE) mean values in the 50°C - 350°C temperature range are reported.

	CTE (α_{th})[1/K]
Sb-doped Mg_2Si (*n*-type legs)	$15.0x10^{-6}$
HMS (*p*-type legs)	$11.1x10^{-6}$
Cu electrical connections	$17.0x10^{-6}$
Aluminium nitride (first considered top ceramic layer)	$4.0x10^{-6}$
Alumina (second considered top ceramic layer)	$8.0x10^{-6}$

Table 2. Coefficients of thermal expansion of the considered materials for the realization of the 16 legs silicide-based TEM.

2. Use of COMSOL Multiphysics® Software

2.1 Governing Equations

To evaluate the mechanical strength of the silicide-based thermoelectric module, it is necessary to consider both heat transfer and solid mechanics equations. According to what reported in the previous section, only thermal conduction has been considered. Thus, the heat transfer in solid and solid mechanics interfaces have been used [5, 6]:

$$\nabla \cdot (-k\nabla T) = Q \qquad (3)$$

$$\nabla \cdot S + F_v = 0 \qquad (4)$$

$$S = C : (\epsilon - \epsilon_{in}) \qquad (5)$$

$$\epsilon_{in} = \epsilon_0 + \epsilon_{th} \qquad (6)$$

$$\epsilon = \frac{1}{2}(\nabla \boldsymbol{u} + (\nabla \boldsymbol{u})^T) \qquad (7)$$

In the heat equation (3), no heat source [W/m^3] was considered: Q=0. In the solid mechanic equations (4) – (7), *S*, *C* and ε are the stress, elasticity and strain tensors respectively. Initial strain ε_0 was considered as discussed in the section 3.2. The term ε_{th} is defined as:

$$\epsilon_{th} = \alpha_{th}(T - T_{ref}) \qquad (8)$$

corresponding to the deformation linked to the thermal expansion coefficient α_{th} [1/K] of materials. In eq. (8), cold side temperature T_c was considered as reference temperature T_{ref}.

2.2 Materials Modeling

In the evaluation of the strength of the thermoelectric module, materials have been considered up to their elastic limit. Beyond this limit, only metal interconnects could present plastic deformations, whereas it is reasonable to expect that thermoelectric legs exhibit brittle behavior, with cracks opening where maximum stress exceeds the elastic limit. Thus, in place of considering localization of plastic deformation, FE analysis has been performed to evaluate where

maximum stress lies outside a safety region, defined through a proper failure criterion. For the thermoelectric elements, Mohr-Coulomb criterion has been considered. According to Mohr-Coulomb criterion, failure is determined by maximum shear stress τ and maximum admissible shear stress is not a constant (Tresca criterion), but linear function of normal stress σ. The straight-line Mohr-Coulomb failure envelope is defined by the equation:

$$|\tau| = c - \sigma tan\phi \qquad (9)$$

where c is the cohesion [N/m^2] and ϕ is the friction angle, both properties of the materials, to be experimentally determined. Mohr-Coulomb failure envelope is plotted in Fig.2 in the {τ, σ} stress plane. Equation (9) means that failure occurs when the principal circle, graphical representation of the local state of stress, is tangent to the curve envelope [7]. Being {σ_1, σ_2, σ_3} the principal stresses, if $\sigma_1 \geq \sigma_2 \geq \sigma_3$, σ_1 and σ_3 are the maximum and minimum stress component. Failure envelope can be written as:

$$\frac{\sigma_1}{f_t} - \frac{\sigma_3}{f_c} = 1 \qquad (10)$$

where f_t and f_c are material strength [N/m^2] in simple tension and compression respectively.

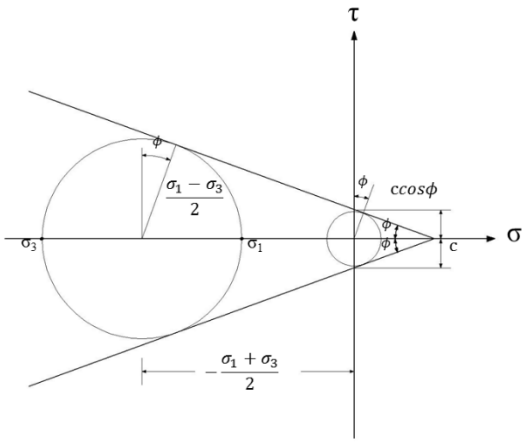

Figure 2. Plot of Mohr-Coulomb failure envelope (9) in the {τ, σ} plane. Failure occur when principal circles are tangent to the curve envelope.

As an alternative option for the evaluation of the strength of thermoelectric legs is to consider maximum normal stress criterion (Rankine). With this approach, failure is expected to occur where maximum tensile stress exceeds f_t or maximum compressive stress exceeds f_c. Since for brittle materials is generally $f_t << f_c$, to consider maximum normal stress criterion is usually to evaluate failure where tensile stress exceeds tensile strength for the material. A comparison between the evaluation of strength of a single *n*-type leg with Mohr-Coulomb and Rankine criteria is presented in the next section. For the strength evaluation of ductile interconnects, yielding was considered to occur where Von Mises stress exceeds a defined yield strength. Ceramic substrates were also expected to undergo brittle failure, but with higher tensile strength (up to 290 MPa for Al_2O_3 [8]). For the simulation, elastic properties of materials were taken as follows (Table 3) [8, 9, 10, 11]:

	Young's modulus *E*[GPa]	Poisson's ratio ν
Sb-doped Mg_2Si (*n*-type legs)	116	0.18
HMS (*p*-type legs)	245	0.2
Cu electrical connections	110	0.35
Aluminium nitride (first considered top ceramic layer)	320	0.22
Alumina (second considered top ceramic layer)	300	0.22

Table 3. Coefficients of thermal expansion of considered materials.

Tensile strength of n-type legs was assumed $f_{t,n}$=80 MPa [10]. In the simulation, this value was considered also for HMS. Ultimate compressive strength of TE legs was taken $f_{c,np}$=140 MPa. For Cu connections, yield strength was assumed $f_{y,c}$=80 MPa and ultimate tensile strength $f_{u,c}$=240 MPa.

3. Results and Discussion

3.1 Single *n*-type leg

At first, simulation on a single 5 x 5 x 7 mm^3 *n*-type leg with ΔT=300 °C has been performed. On both cold and hot sides 300 μm thick metal interconnects were considered. Furthermore, on the top (hot side) a 600 μm thick alumina layer was placed. The surface on the hot side has been constrained with a roller boundary condition. Further limitations of horizontal displacement components have been defined for two points on the top, in order to guarantee convergence to the solution of the static problem (i.e. to guarantee a nonsingular stiffness matrix) without constraining horizontal components of deformation on the top (hot side). A boundary load condition has been defined on the bottom surface (cold side) imposing a pressure q_0=1.0MPa. The simulation has shown that higher stresses occur on the hot side of the thermoelectric leg, because of different dilatation on the horizontal plane of the thermoelectric and the ceramic layer. High tensile stresses (cracks) occur on the corners on the top of the thermoelectric, whereas the inner region of its head potentially undergoes crushing because of high compressive stress. In Fig. 3 the comparison of evaluation of potential failure in the thermoelectric leg with Mohr-Coulomb (MC) and Rankine maximum normal stress (RN) criteria is presented. Blue region (0) stands for elastic region, dark red region (1) stands for plastic/failure region. Stress distribution on slice planes is the same because of symmetry of geometry, loads and constraints. It can be seen that MC criterion leads to wider failure region than RN criterion, since the former imposes a more strict condition on stress (combination of maximum tensile and compressive stress) than the latter (maximum tensile and compressive stress separately considered).

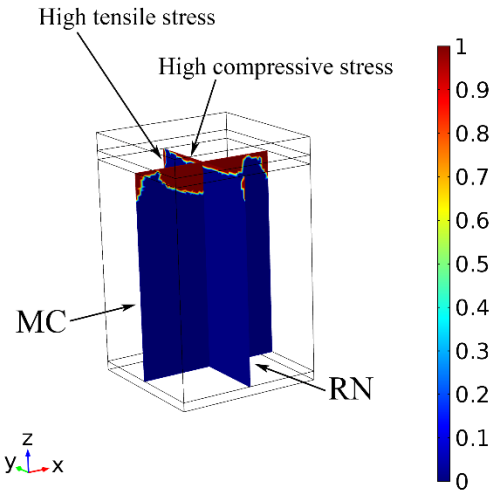

Figure 3. Comparison of evaluation of potential failure in a single *n*-type leg with Mohr-Coulomb (MC, *xz*-plane slice) and maximum normal stress criteria (RN, *yz*-plane slice). Blue (value: 0) depicts the elastic region, dark red (value: 1) depicts the plastic/failure region.

3.2 16 legs TEM

Simulation on a 16 legs silicide-based thermoelectric module with 300 °C temperature gradient was then performed. Dimensions of considered *n*,*p*-type legs are 5 x 5 x 7 mm^3, the thickness of metal connections and top ceramic substrate 300 μm and 600 μm respectively. To take into account that the top metal interconnects have to be soldered to the ceramic layer at high temperature in the first step of the realization of the module, before brazing in a second step these top elements with the TE legs, at lower temperature, an initial strain ε_0 in the ceramic and top interconnects has been defined (see Eq. (6)). This initial strain was considered proportional to the difference between thermal expansion coefficients of connections and ceramic substrate and to the temperature difference between the brazing steps. Boundary load conditions were defined on both hot and cold side with q_0=1.0MPa pressure value. Point constraints have been added to guarantee nonsingular stiffness matrix. Figure 4 reports the evaluation of potential failure in TE legs. Failure is once again evaluated in terms of maximum tensile / compressive stress with reference to Mohr-Coulomb criterion. In this case, alumina was considered for the top ceramic substrate.

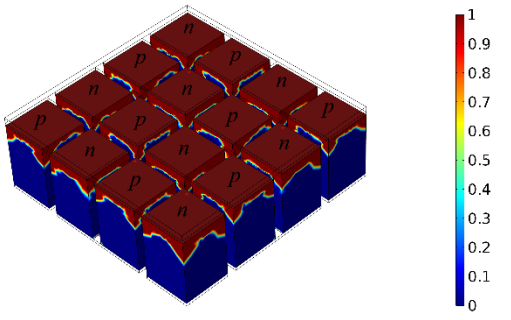

Figure 4. Mohr-Coulomb evaluation of potential failure in TE elements of a 16 legs TEM operating with ΔT=300 °C, with alumina top ceramic substrate. Blue (value: 0) depicts the elastic region, dark red (value: 1) depicts the plastic/failure region.

Failure was found to occur on the top (hot side) of thermoelectric legs where horizontal thermal expansion is limited by less dilating alumina top layer. *N*-type legs presented wider failure regions than *p*-type. In *n*-type elements, higher maximum stresses were found because of higher thermal expansion coefficient. Bending of bottom metal connections is also due to different longitudinal expansion of *n*,*p*-type legs, as shown in Fig. 5.

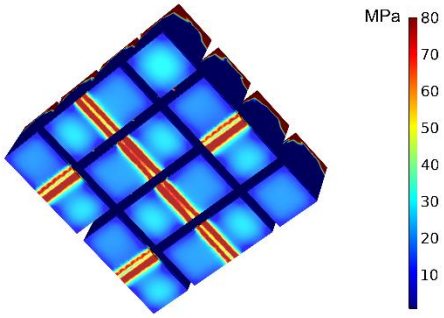

Figure 5. Von Mises stress [MPa] on bending bottom Cu connections. Bending is due to different longitudinal expansion of n and p–type legs.

Considering aluminium nitride instead of alumina for top ceramic layer was found to cause wider damage/failure regions, as shown in Fig. 6.

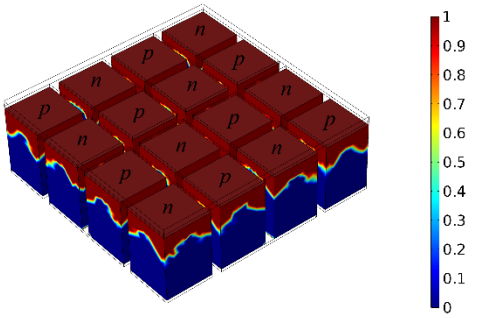

Figure 6. Mohr-Coulomb evaluation of potential failure in the TE legs of the 16 legs prototype with aluminium nitrate instead of alumina as top ceramic layer.

Cracks occurring on the top of thermoelectric legs, on the hot side, has been observed on the 16 legs prototype with the same geometry. Figure 7 shows the Infrared Thermography plot on one side of the thermoelectric module. Highlighted cracks on the heads of *n*-type legs cause discontinuity on temperature profiles [12]. A detail of crack on a *n*-type leg is shown in Fig. 8.

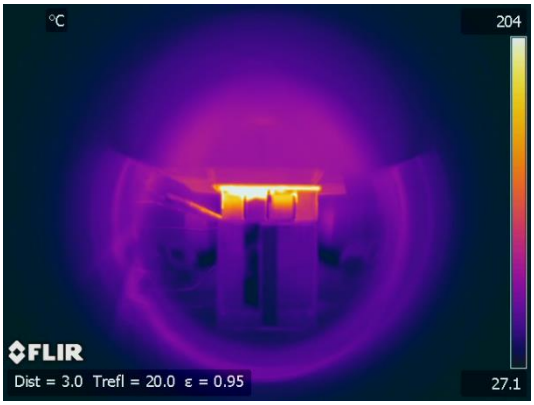

Figure 7. Cracks on n-type legs highlighted through IR Thermography [12].

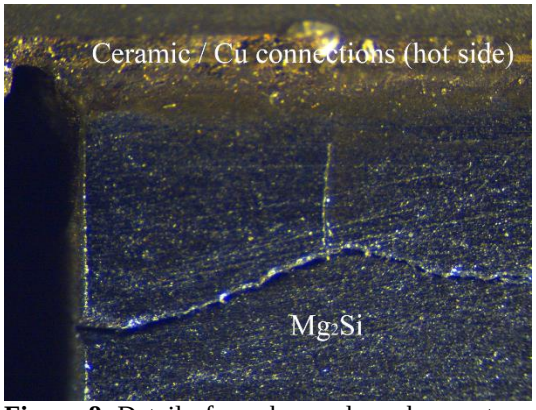

Figure 8. Detail of an observed crack on *n*-type legs.

4. Conclusions

In this work, COMSOL® Multiphysics heat transfer and solid mechanics interfaces have been used to evaluate the strength of a 16 legs module prototype. The strength of the module was considered mainly linked to the strength of thermoelectric elements. Mohr-Coulomb criterion has been chosen to evaluate potential failure regions. Cracks have been found to occur at the top of TE legs on the hot side, where horizontal expansion is limited by the less dilating ceramic layer. In particular, *n*-type legs were found to present higher maximum stresses, as expected because of their higher thermal expansion coefficient in comparison with *p*-type legs. Different thermal expansion of *n* and *p*-type legs was found to cause potential yielding of bottom metal connections. Infrared thermography on a tested module prototype realized with the same geometry has confirmed cracks occurring on the hot side of *n*-type legs. However, in the realized prototype no damage on *p*-type legs has been observed. Thus, to improve the numerical simulation of mechanical behavior of a silicide-based TEM, further informations on ultimate strength of considered materials, in particular higher manganese silicide, are needed. A better characterization of contact between TE legs and metal connections after brazing is furthermore required to evaluate the need to consider soft layers or geometric nonlinearities in the numerical model.

5. References

1. Jaegle M., Simulating Thermoelectric Effects with Finite Element Analysis using COMSOL, *Proceedings of 5th ECT*, Odessa (2007)
2. Miozzo A. et al., Finite Element Approach for the Evaluation and Optimization of Silicide-Based TEG, *Proceedings of 11th ECT*, Noordwijk (2013)
3. Rowe M. D., *Thermoelectrics Handbook Macro to Nano*, CRC Press, Boca Raton (2005)
4. Yasunaga Corporation, http://fine-yasunaga.co.jp/english/index.html
5. COMSOL Multiphysics Documentation, Release 5.0
6. Zienkiewicz O. C. and Taylor R. L., *the Finite Element Method (vol. 2): Solid Mechanics*, 5th ed., Butterworth-Heinemann, Oxford (2000)
7. Chen W. F. and Han D. J., *Plasticity for Structural Engineers*, Springer-Verlag, New York (1988)
8. http://accuratus.com/alumox.html
9. Schmidt R. D. et al., Room-Temperature Mechanical Properties and Slow Crack Growth Behavior of Mg_2Si Thermoelectric Materials, *J Electron Mater*, **Volume 41**, 1210 – 1216 (2012)
10. Sakamoto T. et al., Stress Analysis and Output Power Measurement of an *n*-Mg_2Si Thermoelectric Power Generator with an Unconventional Structure, *J Electron Mater*, Volume 43, 1620 – 1629
11. Chen X., *Synthesis and Thermoelectric Properties of Higher Manganese Silicides for Waste Heat Recovery*, Dissertation Thesis, University of Texas, Austin (2014)
12. Boldrini S. et al., IR Thermography for the Assessment of the Thermal Conductivity of Thermoelectric Modules at Intermediate Temperature, *Proceedings of SPIE 9861* (2016)

6. Acknowledgements

The Authors would like to thank Dr. S. Fasolin for providing the data of thermal expansion coefficient of silicide-based materials considered in this work and Dr. C. Fanciulli for the characterization of ultimate tensile strength of Mg_2Si legs.